Bull Math Biol (2011) 73: 1154–1169
DOI 10.1007/s11538-010-9567-7

ORIGINAL ARTICLE

Evolutionary Behaviour, Trade-Offs and Cyclic and Chaotic Population Dynamics

Andy Hoyle · Roger G. Bowers · Andy White

Received: 5 March 2010 / Accepted: 18 June 2010 / Published online: 17 July 2010

Abstract Many studies of the evolution of life-history traits assume that the underlying population dynamical attractor is stable point equilibrium. However, evolutionary outcomes can change significantly in different circumstances. We present an analysis based on adaptive dynamics of a discrete-time demographic model involving a trade-off whose shape is also an important determinant of evolutionary behaviour. We derive an explicit expression for the fitness in the cyclic region and consequently present an adaptive dynamic analysis which is algebraic. We do this fully in the region of 2-cycles and (using a symbolic package) almost fully for 4-cycles. Simulations illustrate and verify our results. With equilibrium population dynamics, trade-offs with accelerating costs produce a continuously stable strategy (CSS) whereas trade-offs with decelerating costs produce a non-ES repellor. The transition to 2-cycles produces a discontinuous change: the appearance of an intermediate region in which branching points occur. The size of this region decreases as we move through the region of 2-cycles. There is a further discontinuous fall in the size of the branching region during the transition to 4-cycles. We extend our results numerically and with simulations to higher-period cycles and chaos. Simulations show that chaotic population dynamics can evolve from equilibrium and vice-versa.

A. Hoyle (✉)
Department of Computing Science and Mathematics, University of Stirling, Stirling, FK9 4LA, UK
e-mail: ash@maths.stir.ac.uk

R.G. Bowers
Department of Mathematical Sciences, The University of Liverpool, Liverpool, L69 3BX, UK
e-mail: sx04@liverpool.ac.uk

A. White
Department of Mathematics and the Maxwell Institute for Mathematical Sciences,
Heriot Watt University, Edinburgh, EH14 4AS, UK
e-mail: A.R.White@hw.ac.uk

Keywords Adaptive dynamics · Trade-offs · Logistic equation · Evolutionary branching · Chaos

1 Introduction

Adaptive dynamics (Metz et al. 1996; Geritz et al. 1998) allows the study of trait substitution sequences resulting from the challenge of a resident strain by a closely similar variant. Commonly, in applications, the following two features are found.

First, the underlying population dynamical state is restricted to equilibrium—despite the fact that ecological systems exhibit a range of complex population dynamics, such as periodic and quasi-periodic cycles and chaos (Katok and Hasselblatt 1995), that simple models can capture this behaviour (Gurney and Nisbet 1998; Cushing et al. 2003) and adaptive dynamics is suitable to analyse evolution under non-equilibrium dynamics. Exceptions, which do consider non-equilibrium behaviour, include recent work by White et al. (2006) and Geritz et al. (2007) and a body of work focussed on the question of whether evolution leads to equilibrium or non-equilibrium dynamics (Gatto 1993; Ferriere and Gatto 1993; Doebeli and Koella 1995; Ebenman et al. 1996; Greenman et al. 2005).

The second feature frequently present is that the role of trade-offs between evolving parameters is not discussed—despite the fact that these are central to evolutionary theory, arising as they do, when the evolution of particular fitness traits is constrained deterministically by other traits such that a benefit in one results in a cost in another (Stearns 1992; Roff 2002). Exceptions, which do consider trade-offs explicitly, include classical life-history theory (Levins 1962; Schaffer 1974; Stearns 1992; Roff 2002) and more recent adaptive dynamics studies that consider arbitrarily shaped trade-offs (Boots and Haraguchi 1999; Kisdi 2001; Bowers et al. 2003; De Mazancourt and Dieckmann 2004; White and Bowers 2005; Geritz et al. 2007; Svennungsen and Kisdi 2009; Boldin et al. 2009). It is noteworthy that new geometric methods for analysing adaptive dynamics (De Mazancourt and Dieckmann 2004; Rueffler et al. 2004; Bowers et al. 2005) stress the importance of trade-offs.

In this article, we provide an adaptive dynamics analysis which is free from the above 'restrictions'—the analysis includes non-equilibrium (cyclic) population dynamics and investigates the role of trade-offs explicitly. A novelty is that, for our given model, we derive an explicit algebraic expression for the fitness in the cyclic region and consequently present an adaptive dynamic analysis (fitness derivatives and their consequences for singular behaviour) which itself is algebraic. This contrasts with the previous work of White et al. (2006) which used numerical and simulation based techniques. (Of course, we use simulation to illuminate the present work.)

The algebraic results available here allow a detailed investigation of the applicability of the results relating underlying population dynamics and trade-off type to evolutionary behaviour. They allow us to determine whether changes in the underlying dynamics alter the evolutionary outcome and to define precisely the regions (in terms of trade-off shape) in which different evolutionary behaviour is exhibited. Our findings can also be compared with those of White et al. (2006) which indicated that low amplitude, non-equilibrium dynamics would not alter the evolutionary results

applicable to equilibrium but that, beyond a threshold-amplitude, new behaviour (for example, branching points) appears.

In the following sections, we introduce our population dynamical model and discuss its biological context; we present an adaptive dynamical analysis in the point equilibrium region, we present a similar algebraic analysis—fitness, fitness derivatives, location and nature of evolutionary singularities—in the cyclic region (for period two cycles); we investigate when new evolutionary behaviour (branching points) occurs and associated limit behaviour in the parameter space of our model; we extend this algebraic analysis almost fully to the region of 4-cycles (using a symbolic package); we illustrate and verify our results with simulations; for higher-period cycles and chaos we rely on numerical studies and simulations; we finish with a discussion.

2 The Model

The biological context we discuss here is the reproduction and survival of individuals of a single species with density x_t at time t. The discrete time population dynamics is given as

$$x_{t+1} = r x_t (1 - q x_t) + s x_t, \tag{1}$$

where r is the low density reproduction ratio whilst (non-zero values of) the parameter q yield density-dependence in reproduction; s is the survival probability. (Density dependence acting on survival could be included with little change.) We consider an explicit trade-off between reproduction and survival of the form $s = f(r)$. This model is similar to the 'exponential' model of White et al. (2006) but its logistic form allows an algebraic analysis missing in this previous paper.

3 Adaptive Dynamics

3.1 Fitness—Stable Point Equilibrium

For a general dynamics of the form

$$x_{t+1} = M(r, x_t) x_t, \tag{2}$$

a point equilibrium satisfies $x_{t+1} = x_t = x_p$. The fitness of a mutant with trait $\tilde{r}$ attempting to invade a demographically stable resident equilibrium population $x_p(r)$ with trait r is given by Metz et al. (1992)

$$w(\tilde{r}, r) = \ln\big[M\big(\tilde{r}, x_p(r)\big)\big]. \tag{3}$$

(The function M is positive in our context.)

For our model

$$x_P = x_p(r) = \frac{r + f(r) - 1}{qr}, \tag{4}$$

which incorporates the trade-off $s = f(r)$. The parameter region of interest is $1 < r + f(r) < 3$ where this is stable (and the extinction equilibrium is not) (May 1975).

This gives

$$w(\tilde{r},r) = \ln\left[\tilde{r}(1-qx_P) + f(\tilde{r})\right] = \ln\left[\frac{(1-f(\tilde{r}))(1-f(r))}{r}\left(\frac{\tilde{r}}{1-f(\tilde{r})} - \frac{r}{1-f(r)}\right) + 1\right]. \quad (5)$$

The solutions r^* of $\partial w/(\partial \tilde{r})|_{\tilde{r}=r} = 0$ are evolutionary singularities; here this condition yields

$$f'(r^*) = \frac{f(r^*)-1}{r^*}. \quad (6)$$

The second derivatives of the fitness evaluated at the singularity reveal the nature of the singularity (Metz et al. 1996; Geritz et al. 1998); here this leads to conditions: r^* is evolutionary stable (ES) if $f''(r^*) < 0$ and is convergent stable (CS) if $f''(r^*) < 0$. Hence we have an evolutionary attractor, or continuously stable strategy (CSS), (both ES and CS) for trade-offs with accelerating costs, $f''(r^*) < 0$, and a repellor (neither ES nor CS) for trade-offs with decelerating costs, $f''(r^*) > 0$. This is consistent with (5) which shows that evolution optimises $r/(1-f(r))$ (the reproduction ratio at low densities divided by the death ratio).

3.2 Fitness—Stable Cycles

After τ steps of the above generalised discrete dynamics, we have

$$x_{t+\tau} = M(r, x_{t+\tau-1}) \times \cdots \times M(r, x_{t+2})M(r, x_{t+1})M(r, x_t)x_t. \quad (7)$$

Suppose there is a stable τ-cycle

$$x_0(r), x_1(r), \ldots, x_{\tau-1}(r); \quad (8)$$

the appropriate definition of fitness (Eckmann and Ruelle 1985; Metz et al. 1992; Ferriere and Gatto 1993) is

$$w(\tilde{r},r) = \frac{1}{\tau}\ln\left[M\left(\tilde{r}, x_{\tau-1}(r)\right) \times \cdots \times M\left(\tilde{r}, x_2(r)\right)M\left(\tilde{r}, x_1(r)\right)M\left(\tilde{r}, x_0(r)\right)\right]. \quad (9)$$

3.3 Our Model—Stable 2-Cycles

We now proceed with a fully algebraic calculation of the fitness and its derivatives for resident (and mutant) 2-cycles in our model. This allows us to determine the location and nature of the evolutionary singularities in this demographic regime and to compare these with those in the point stable region. In particular, since 2-cycles are stable for $(3 < r + f(r) < 1 + \sqrt{6})$ (May 1975), we can investigate the behaviour near the change at $r + f(r) = 3$.

The fitness is

$$w(\tilde{r},r) = \frac{1}{2}\ln\left[M\left(\tilde{r}, x_1(r)\right)M\left(\tilde{r}, x_0(r)\right)\right], \quad (10)$$

where, for $i = 0, 1$,

$$M\big(\tilde{r}, x_i(r)\big) = M_i = \tilde{r}\big(1 - q x_i(r)\big) + f(\tilde{r}). \tag{11}$$

To apply this we need information on $x_i(r)$. With a little algebraic manipulation, the fitness expression can be written in terms of the sum and product of the densities $x_i(r)$ which can be determined explicitly (see Appendix A). This allows the derivative of the fitness function to be determined, and by setting $\partial w(\tilde{r}, r)/\partial \tilde{r} = 0$ with $\tilde{r} = r = r^*$ this gives the locations of the evolutionary singularities as the solutions of

$$f'(r^*) = \frac{f(r^*)}{r^*} - \frac{2}{r^*(r^* + f(r^*) - 1)}. \tag{12}$$

(As expected, as $r + f(r) \to 3$, this condition for the evolutionary singularities tends to $f'(r^*) = (f(r^*) - 1)/r^*$, which is the condition in the point equilibrium regime found above.)

The second derivative of the fitness with respect to the mutant parameter $\tilde{r}$ and the mixed derivative, both evaluated at the singularity, can also be determined explicitly (see Appendix A) and it transpires that the conditions for the singularity to be ES and CS are as follows (Metz et al. 1996; Geritz et al. 1998):

$$\text{ES: } f''(r^*) < \frac{2}{r^{*2}(r^* + f(r^*) - 1)} - \frac{8}{r^{*2}(r^* + f(r^*) - 1)^3} \tag{13}$$

$$\text{CS: } f''(r^*) < \frac{2}{r^{*2}(r^* + f(r^*) - 1)} - \frac{8}{r^{*2}(r^* + f(r^*) - 1)^3} + \frac{2(r^* + f(r^*) + 1)}{r^{*2}(r^* + f(r^*) - 1)^3}. \tag{14}$$

(Stability of the cycles certainly ensures that $r^* + f(r^*) - 1 > 0$.) Again the system can evolve towards an evolutionary attractor (ES and CS inequalities satisfied), or away from the singularity (neither ES nor CS inequalities satisfied). However, now there is a possibility of a third evolutionary outcome, that of evolutionary branching. This behaviour occurs when the curvature of the trade-off is such that the singularity is CS but not ES (recall again that $r^* + f(r^*) - 1 > 0$).

3.4 Size of the Branching Region

We have shown that, when the demographic attractor is a 2-cycle, evolutionary branching is possible, whereas for stable point equilibria only evolutionary attractors and repellors are possible. For 2-cycles, branching is possible when the second derivative of the trade-off function evaluated at the singularity, $f''(r^*)$, exceeds the right-hand side of (13) but is less than the right-hand side of (14). We measure this range of values using

$$B = \frac{2(r^* + f(r^*) + 1)}{r^{*2}(r^* + f(r^*) - 1)^3}. \tag{15}$$

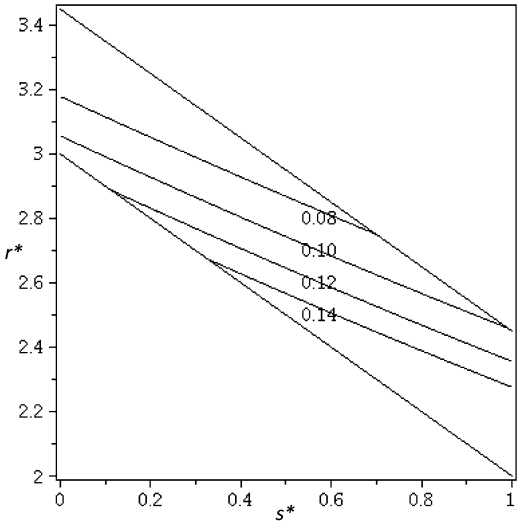

Fig. 1 Contour map of the range of magnitudes of $f''(r^*)$ for which branching occurs against the singular values of r^* and $s^* = f(r^*)$, for the region where 2-cycles occur $(3 < r^* + s^* < 1 + \sqrt{6})$

To study how the possibility of branching changes with r^* and $s^* = f(r^*)$ we plot a contour map, of B for the region of 2-cycles (Fig. 1). From this we see that as $r^* + f(r^*)$ increases, the range of values of $f''(r^*)$ for which branching occurs decreases. Using the result from (A.9) of Appendix A this shows that as the normalised amplitude of the evolutionarily singular population cycle increases, the range of values $f''(r^*)$ for which branching occurs diminishes.

3.5 Behaviour Near the Transition to Cycles

It follows from the above that branching is more likely just after the transition to 2-cycles than at higher values of $r^* + f(r^*)$ in the 2-cycle region. Since branching is not possible in the point stable region below the transition, anomalous limiting behaviour is suggested. We investigate this next.

In the limit $r^* + f(r^*) \to 3$, the condition for the 'cyclic' singularity to be ES (13) approaches $f''(r^*) < 0$, which matches the condition that the stable point equilibrium obtains. However, the condition for the cyclic singularity to be CS (14) approaches $f''(r^*) < 1/r^{*2}$ in this limit, which differs from the condition $f''(r^*) < 0$ for stable point equilibrium. This is the origin of the discontinuity in the evolutionary outcomes.

We illustrate in Fig. 2(a) how the magnitudes of the $f''(r^*)$ satisfying the ES and/or CS conditions change as we increase r^*. The figure applies for any trade-off function with the given values of $s^* = f(r^*)$ (here 0.6) and $f'(r^*)$ (from (12)). We plot the right hand side of the inequalities (13) and (14) for the evolutionary properties; the conditions are satisfied below the respective lines. The discontinuity in the CS condition is clear; although the curve representing the ES condition is continuous, it is not smooth due to the discontinuity in the gradient.

The above discontinuities reflect the following behaviour of the densities as the transition is approached from the cyclic region: although $x_a + x_b \to 2x_p$ and $x_a x_b \to x_p^2$ (which apply in particular for evolutionary singularities), we find that

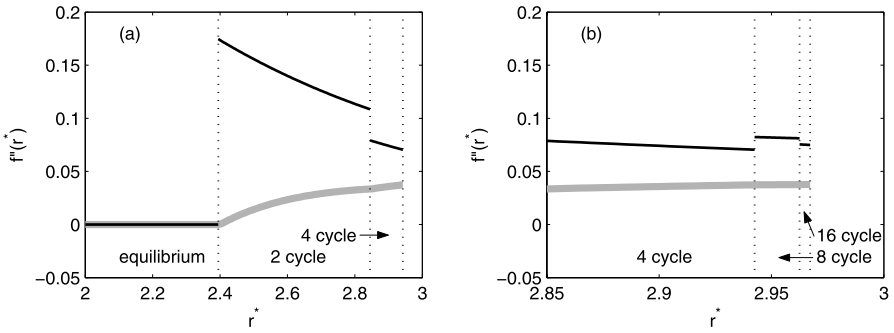

Fig. 2 Plot of r^* against the required magnitude of $f''(r^*)$ needed to a satisfy the evolutionary properties ES (*thick grey line*) and CS (*solid black line*) for any trade-off function with $s^* = f(r^*) = 0.6$ and (**a**) $f'(r^*)$ determined using (12) in the 2 cycle region and as described in Appendix A in the 4 cycle region; (**b**) the boundaries are determined using a numerical procedure as outlined in Appendix B. For $f''(r^*)$ below the ES line the singularity is an evolutionary attractor, above the CS line it is an evolutionary repellor and between the ES and CS line (if possible) it is a branching point

$\partial(x_a + x_b)/\partial r|_* \to -2/qr^{*2}$ and $\partial(x_a x_b)/\partial r|_* \to -6/qr^{*2}$ whilst $\partial(x_p)/\partial r|_* \to 0$. Results depending on these derivatives show discontinuity; we observe from the above that the CS boundary does depend on these derivatives—and hence is discontinuous; the ES boundary does not depend on these derivatives (it involves partial derivatives with respect to the mutant trait only)—and hence is continuous; however, its derivative, with respect to r^*, does depend on the above derivatives—and hence is discontinuous.

3.6 Our Model—Stable 4-Cycles

In the 4-cycle region, the fitness (10) is replaced by

$$w(\tilde{r}, r) = \frac{1}{4} \ln\big[M\big(\tilde{r}, x_3(r)\big) M\big(\tilde{r}, x_2(r)\big) M\big(\tilde{r}, x_1(r)\big) M\big(\tilde{r}, x_0(r)\big)\big]. \tag{16}$$

The rest of the analysis can be completed largely algebraically using an appropriate symbolic package (Maple v.13); it is only necessary to ascribe values to r^* and $s^* = f(r^*)$. The 4-step recurrence relation replacing (A.3) is of degree 16 and cannot be handled algebraically; however, numerical values of the appropriate roots can be found at the singularity (we take $q = 1$). The 4 roots corresponding to the point equilibria and 2-cycle can then be removed leaving in the 4-cycle region of the period-doubling cascade exactly 4 other real roots corresponding to the new cycle; these can be used wherever necessary in the following. Apart from this we can proceed algebraically. The first derivative $\partial w(\tilde{r}, r)/\partial \tilde{r}$ of the fitness can be found from (16). Evaluating this at the singular point gives an expression with only $f'(r^*)$ unknown. Since this expression must be zero, we can solve for $f'(r^*)$. The mixed and second derivatives equivalent to (A.12) and (A.14) can now be found algebraically and inequalities for $f''(r^*)$ parallelling (13) and (14) established. These inequalities require the known values of $f(r^*)$ and $f'(r^*)$. They also require (compare (A.14)) values of density derivatives at the singularity. As claimed above, these do not have

to be found by numerical differentiation; the equilibrium equation for the 4-step recurrence relation can be (implicitly) differentiated algebraically and solved for the density derivative, yielding an expression involving the density itself.

Proceeding in the above way, we obtain the results shown in Fig. 2(a) for 4-cycles. Similar discontinuities in the boundaries arise at the transition to 4-cycles as were found at the previous transition. Branching behaviour is less likely for any r^* in the 4-cycle region than it is anywhere in the 2-cycle region and, in parallel with previous findings, the size of the branching region in terms of $f''(r^*)$ falls (slightly) as r^* (and consequently the amplitude of the oscillations) increases through the region of 4-cycles.

3.7 Beyond the 4-Cycle Region

It is not possible to compute the ES and CS boundaries algebraically beyond the 4-cycle region, but it is possible to use numerical procedures to approximate these boundaries for higher period cycles (see Appendix B). The numerically computed ES and CS boundaries are shown for the 4, 8 and 16-cycle region in Fig. 2(b). There is a very close comparison between the algebraic and numerical boundaries in the 4-cycle region, and familiar discontinuities in the CS boundary are exhibited at the transition between cycle regions. Note the CS boundary can increase at the discontinuity as shown by the transition between 4 to 8-cycles. Note also the likelihood of cycles consistently decreases across each cycle region. Extending the numerical methods beyond the 16 cycle region into the chaotic region is not possible as the method requires a consistent population dynamic attractor in the neighbourhood of the singular point and this does not occur when the dynamics are chaotic.

In Fig. 3, we illustrate the behaviour in Fig. 2 by giving the results of related multi-strain simulations (see Appendix C) using a representative trade-off. In Fig. 3(a)–(c) and 3(d)–(f) we illustrate simulations that lead to evolutionary attractors. In both cases, the simulation indicates that the evolving parameter r will be attracted towards and become fixed at the singular value r^*. Notice, however, that trade-offs can be chosen such that underlying population dynamics at r^* can exhibit a range of behaviour. In Fig. 3(a)–(c), as the system evolves the population dynamics evolve from chaotic to become fixed at equilibrium behaviour. In Fig. 3(d)–(f), the reverse occurs as the system evolves the dynamics progress from equilibrium through the period doubling cascade to chaos. Trade-offs can be chosen such that any of the possible underlying dynamics are exhibited at r^* when it is an evolutionary attractor. In Fig. 3(g)–(i), we illustrate a simulation of the behaviour when the singular point is an evolutionary repellor. Here starting near the singular point the system evolves away to either the maximum or minimum value permitted by the trade-off (depending on whether the initial strain was above or below the singular point, respectively). The underlying population dynamics change according to the evolving value of the parameters and become fixed on the dynamics associated with either the maximum or minimum value on the trade-off (the minimum value is attained in Fig. 3(g)–(i)).

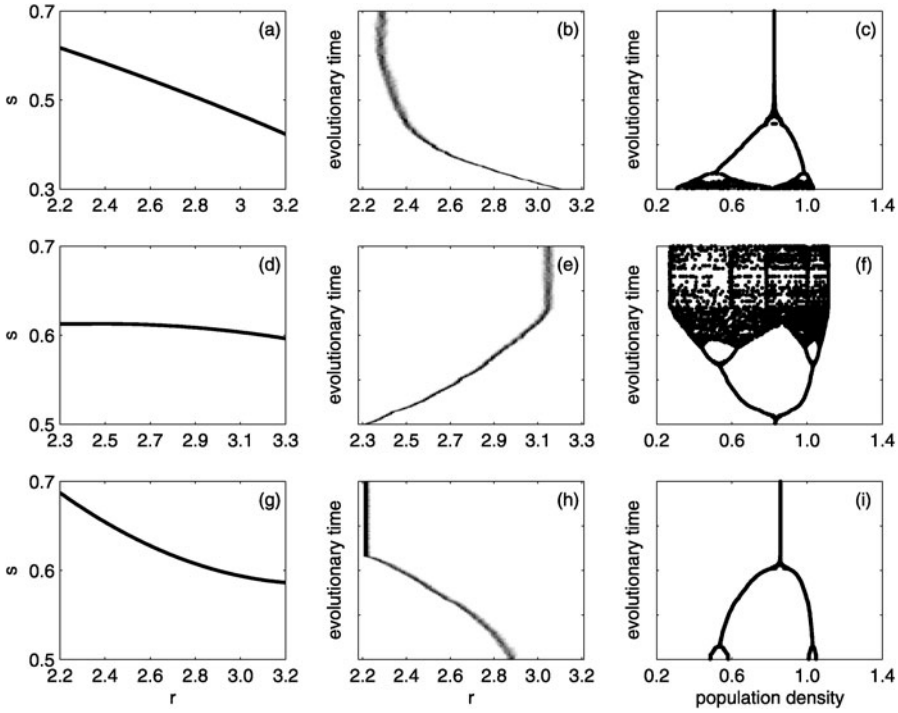

Fig. 3 The trade-off in (**a**) leads to an evolutionary attractor shown in the simulation (**b**). The underlying population dynamics as the value of r (and $s = f(r)$) evolves in (**b**) are shown in (**c**) with dynamics changing from chaotic to periodic cycles to equilibrium at the attractor. Here the trade-off is $s = -0.025r^2 - 0.0589r + 0.8678$ which produces a singular point at $r = 2.3$ with $f''(r) = -0.05$. The trade-off in (**d**) leads to an evolutionary attractor shown in the simulation (**e**) and the underlying population dynamics as the value of r evolves in (**e**) are shown in (**f**) with dynamics changing from equilibrium through the period doubling cascade to chaos. Here the trade-off is $s = -0.025r^2 + 0.1243r + 0.4583$ which produces a singular point at $r = 3.15$ with $f''(r) = -0.05$. The trade-off in (**g**) leads to an evolutionary repellor shown in the simulation (**h**) and the underlying population dynamics as the value of r evolves in (**h**) are shown in (**i**) with dynamics changing from 4-cycles to 2-cycles to equilibrium. Here the trade-off is $s = 0.08r^2 - 0.533r + 1.4728$ which produces a singular point at $r = 2.9$ with $f''(r) = 0.16$

In Fig. 4, we illustrate the behaviour when the singular point leads to evolutionary branching. In Fig. 4(a)–(d) branching occurs when the underlying population dynamics exhibit a 2-cycle. The population dynamics in each of the subsequent branches also exhibit 2-cycles (Fig. 4(c)–(d)). A similar result occurs when branching occurs with chaotic underlying dynamics with the separate branches also continuing to exhibit chaos (Fig. 4(e)–(h)). Note that the population dynamics in the branches would be very different if they existed in isolation. For both of the examples shown in Fig. 4, the left branch would exhibit equilibrium dynamics and the right branch chaos. It is interesting to observe that at evolutionary branching points the population dynamics in the branched populations exhibit the same behaviour as that displayed immediately prior to branching. We observed this behaviour in all cyclic and chaotic regions but it requires further investigation (beyond the scope of this study) to determine whether this is a general property.

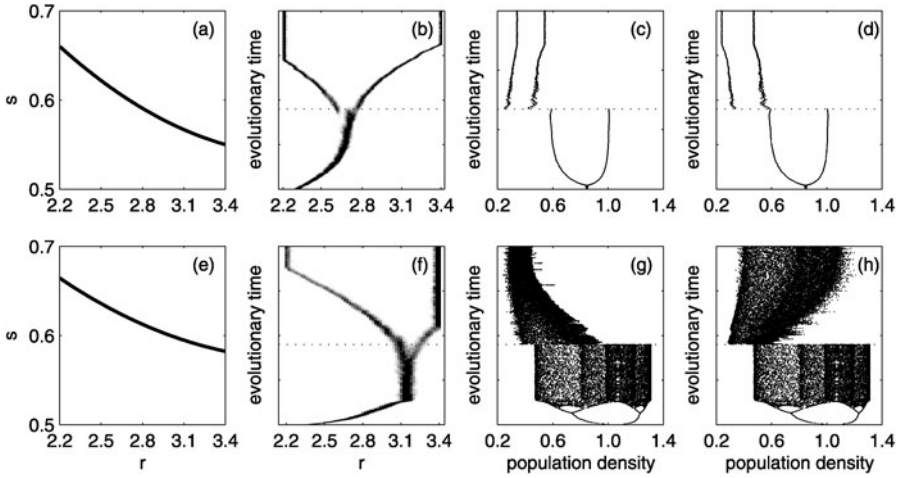

Fig. 4 The trade-off described in (**a**) leads to evolutionary branching as shown in the simulation (**b**) and branching occurs when the underlying population dynamics exhibit a 2-cycle. Figures (**c**) and (**d**) are identical below the *dotted line* and display the population dynamics as r (and $s = f(r)$) evolves in (**b**). Above the *dotted line* in (**b**) evolutionary branching has occurred and (**c**) follows the population dynamics exhibited by left branch and (**d**) follows the population dynamics exhibited by the right branch. Here the trade-off is $s = 0.04r^2 - 0.3158r + 1.1612$ which produces a singular point at $r = 2.7$ with $f''(r) = 0.08$. The panels (**e**)–(**h**) are analogous but the trade-off has been chosen such that branching occurs when the underlying population dynamics are chaotic. Here the trade-off is $s = 0.03r^2 - 0.2364r + 1.0392$ which produces a singular point at $r = 3.15$ with $f''(r) = 0.06$

4 Discussion

We have discussed the adaptive dynamics associated with a discrete time demographic model in a context where there is a trade-off between parameters modelling reproduction and survival of individuals. Unusually, the model admits algebraic analysis (fitness and its appropriate derivatives) not only when the underlying dynamics is equilibrium but also when it is cyclic of period two. For (stable) equilibrium population dynamics the shape of the trade-off characterises evolutionary behaviour in a simple fashion: trade-offs with accelerating costs correspond to attractors, or continuously stable strategies (CSS), (ES and CS); trade-offs with decelerating costs correspond to repellors (not ES and not CS). For cyclic population dynamics of period 2 an extension of this is found: trade-offs with accelerating or weak decelerating costs correspond to attractors; trade-offs with strong decelerating costs correspond to repellors and now trade-offs which are intermediate between these are associated with branching points (not ES but CS). Underlying branching behaviour is cyclic dynamics. The range of values of the second derivative of the trade-off in the intermediate region associated with branching points is largest close (in parameter space) to the transition from equilibrium to cyclic demography and decreases as we move further into the cyclic region. Additionally, the (normalised) amplitude of the oscillations increases as we move through the 2 cycle region—thus branching points are more likely with low amplitude oscillations.

In the case where the underlying population dynamical state is a 4-cycle, the above procedure for two cycles can still be completed almost entirely algebraically using a suitable computer package. Only, one step has to be numerical—this is the identification of the 4-cycle densities corresponding to the given singular values r^* and $s^* = f(r^*)$. The results in the 4-cycle region mirror those in the 2-cycle region regarding the relationship between evolutionary behaviour and the value of the second derivative $f''(r^*)$. Moreover, branching behaviour is less likely for any r^* in the 4-cycle region than it is anywhere in the 2-cycle region.

To study more of the period doubling cascade in this manner is not feasible, but a numerical scheme can be implemented to compute the boundaries for higher period cycles (Fig. 2(b)). The ES boundary increases continuously (but not smoothly) as r^* increases and the CS boundary displays discontinuous jumps at each period doubling of the underlying population cycles. At the boundary between 4-cycles and 8-cycles, there is a discontinuity in the CS boundary but branching becomes more likely. The discontinuous jump in the CS boundary between 8-cycles to 16 cycles implies that branching becomes less likely. However, in all cases the CS boundary decreases as we move through each individual cyclic region. The above findings run counter to those reported in White et al. (2006) on the basis of simulation studies of a different but related model. These authors find that for non-equilibrium dynamics with low amplitude population oscillations the evolutionary behaviour is as for equilibrium dynamics (which is the same as the evolutionary behaviour reported for equilibrium populations dynamics here). White et al. (2006) report that it is when the magnitude of the population oscillations exceeds a threshold that branching is observed. The Ricker type density-dependence effect (a negative exponential function) means that it is not possible to produce analytical results for the model defined in White et al. (2006). However, future research should be aimed at reconciling the present findings and those of White et al. (2006), understanding how the nature of self-regulation impacts on evolutionary behaviour and therefore providing a broader perspective of how population dynamics affect the evolutionary outcomes in ecological models.

The current study can also be used to further inform the debate on whether evolution leads to selection for equilibrium or more complicated (oscillatory, chaotic) population dynamics. Laboratory experiments on Drosophila melanogaster have indicated that stable population dynamics may result from individual selection acting on demographic parameters (Prasad and Joshi 2003) and conversely have reported that there is either no evolution of population stability, or very slow change (Mueller et al. 2000). There is also a lack of consensus in theoretical studies (based on similar discrete time population models to the logistic model presented here) used to address this debate; some studies indicate that equilibrium underlying population dynamics are most likely to result from selection of life-history traits (Gatto 1993; Doebeli and Koella 1995; Ebenman et al. 1996) and others suggest that oscillatory or chaotic dynamics are most likely or that the outcome depends on the shape of the set of feasibility for specific parameters (Gatto 1993; Ferriere and Gatto 1993). Such feasibility sets are related to life-history trade-offs and our study highlights how the outcome can be determined by the shape of the trade-off (Fig. 3). An evolutionary attracting singular point can occur for parameters that lead to either equilibrium, oscillatory or chaotic dynamics and it is noteworthy that such trade-offs have (visually) similar cost structures, yet selection leads to very different population dynamics.

When the singular point is a repellor, evolution tends to select for either the minimum or maximum trait value (depending on the position of the initial trait in relation to the singular point) and again any type of population dynamics could occur at these values. When evolutionary branching occurs, the situation is more complicated.

It is always crucial to remember that evolutionary behaviour of a system can change dramatically when the underlying population dynamics change from being at equilibrium to an unstable state, for example, to a stable 2-cycle. More importantly is the way this change occurs. It should not be assumed there is a gradual change during the transition as it has been shown that this assumption can be spectacularly incorrect and that the possibility of branching points (size of the branching region with respect to the shape of the trade-off), and speciation, occurring is greatest at the transition from the population being stable to that of 2-cycles, and that this is where the population cycles are the smallest!

Acknowledgements A.W. is supported by a Royal Society of Edinburgh and Scottish Government Support Research Fellowship.

Appendix A

The fitness is

$$w(\tilde{r}, r) = \frac{1}{2}\ln\big[M\big(\tilde{r}, x_1(r)\big)M\big(\tilde{r}, x_0(r)\big)\big], \tag{A.1}$$

where, for $i = 0, 1$,

$$M\big(\tilde{r}, x_i(r)\big) = M_i = \tilde{r}\big(1 - qx_i(r)\big) + f(\tilde{r}). \tag{A.2}$$

To apply this we need information on the $x_i(r)$.

We have

$$\begin{aligned} x_{t+2} = {} & r\big(rx_t(1-qx_t) + f(r)x_t\big)\big(1 - q(rx_t(1-qx_t) + f(r)x_t)\big) \\ & + f(r)\big(rx_t(1-qx_t) + f(r)x_t\big). \end{aligned} \tag{A.3}$$

Using the property $x_{t+2} = x_t = x_i$ of a 2-cycle, this gives

$$x_i(x_i - x_P)\big(x_i^2 - bx_i + c\big) = 0. \tag{A.4}$$

Here x_P is given by the formula for point equilibrium (4), and the solution of the quadratic gives two values corresponding to the 2-cycle, which we denote x_a and x_b. Explicitly, the quadratic is

$$x_i^2 - \frac{r + f(r) + 1}{rq}x_i + \frac{r + f(r) + 1}{r^2q^2} = 0. \tag{A.5}$$

Since the fitness

$$w(\tilde{r}, r) = \frac{1}{2}\ln\big[\big(\tilde{r} + f(\tilde{r})\big)^2 - q\tilde{r}\big(\tilde{r} + f(\tilde{r})\big)(x_a + x_b) + q^2\tilde{r}^2x_ax_b\big], \tag{A.6}$$

only depends on the sum and product of x_a and x_b, we shall not need explicit forms for the roots; the results

$$x_a + x_b = \frac{r + f(r) + 1}{qr} \tag{A.7}$$

and

$$x_a x_b = \frac{r + f(r) + 1}{q^2 r^2} \tag{A.8}$$

suffice. Note that the normalised square of the amplitude of the oscillations

$$\frac{(x_a - x_b)^2}{(\frac{1}{2}(x_a + x_b))^2} = \frac{(x_a + x_b)^2 - 4x_a x_b}{(\frac{1}{2}(x_a + x_b))^2} = \frac{4(r + f(r) - 3)}{(r + f(r) + 1)} \tag{A.9}$$

increases with $r + f(r)$. Furthermore, at the cross-over of stability (point equilibrium to 2-cycle), i.e. as $r + f(r) \to 3$, the difference between x_a and x_b approaches zero and $x_a + x_b \to 2x_p$. Correspondingly, $x_a \,\&\, x_b \to x_p$.

The first derivative of the fitness with respect to the mutant can be expressed as

$$\frac{\partial w(\tilde{r}, r)}{\partial \tilde{r}} = \frac{2(\tilde{r} + f(\tilde{r}))(1 + f'(\tilde{r})) - q(2\tilde{r} + f(\tilde{r}) + \tilde{r} f'(\tilde{r}))(x_a + x_b) + 2q^2 \tilde{r} x_a x_b}{2M_a M_b}, \tag{A.10}$$

where $M_a M_b = (\tilde{r} + f(\tilde{r}))^2 - q\tilde{r}(\tilde{r} + f(\tilde{r}))(x_a + x_b) + q^2 \tilde{r}^2 x_a x_b$ as above is the positive denominator. Setting this derivative equal to zero, with $\tilde{r} = r = r^*$, and using results above for $x_a + x_b$ and $x_a x_b$ gives the locations of the evolutionary singularities as the solutions of

$$f'(r^*) = \frac{f(r^*)}{r^*} - \frac{2}{r^*(r^* + f(r^*) - 1)} \tag{A.11}$$

which is the condition stated in (12).

The second derivative of the fitness with respect to the mutant parameter $\tilde{r}$ evaluated at the singularity is

$$\begin{aligned} \left.\frac{\partial^2 w}{\partial \tilde{r}^2}\right|_{r^*} = \frac{1}{2M_a M_b}\big\{ & f''(r^*)\big[2f(r^*) + r^*\big(2 - q(x_a + x_b)\big)\big] \\ & + 2\big[1 - q\big(1 + f'(r^*)\big)(x_a + x_b) \\ & + f'(r^*)^2 + q^2 x_a x_b + 2f'(r^*)\big]\big\}. \end{aligned} \tag{A.12}$$

(Take $M_a M_b$ to be evaluated at the singularity wherever necessary.) This can be simplified to

$$\left.\frac{\partial^2 w}{\partial \tilde{r}^2}\right|_{r^*} = \frac{1}{2M_a M_b}\left[f''(r^*)\big(r + f(r) - 1\big) - \frac{2}{r^2} + \frac{8}{r^2(r + f(r) - 1)^2}\right]. \tag{A.13}$$

To find the condition for convergence stability (CS), we need the mixed derivative of the fitness; we find

$$\left.\frac{\partial^2 w}{\partial r\,\partial \tilde{r}}\right|_{r^*} = \frac{1}{2M_aM_b}\Big[-q\big(2r^* + f(r^*) + r^* f'(r^*)\big)\left.\frac{\partial}{\partial r}(x_a + x_b)\right|_{r^*} + 2q^2 r^* \left.\frac{\partial}{\partial r}(x_a x_b)\right|_{r^*}\Big]. \tag{A.14}$$

To simplify this requires the derivatives

$$\frac{\partial(x_a + x_b)}{\partial r} = \frac{rf'(r) - f(r) - 1}{qr^2}, \tag{A.15}$$

$$\frac{\partial(x_a x_b)}{\partial r} = \frac{(rf'(r) - f(r) - 1) - (r + f(r) + 1)}{q^2 r^3}. \tag{A.16}$$

Using these, evaluated at the evolutionary singularity, the mixed derivative can be simplified to

$$\left.\frac{\partial^2 w}{\partial \tilde{r}\,\partial r}\right|_{r^*} = \frac{1}{2M_aM_b}\left[-\frac{2(r^* + f(r^*) + 1)}{r^{*2}(r^* + f(r^*) - 1)^2}\right]. \tag{A.17}$$

Hence, as stated in (13)–(14), the conditions for each of the properties of the singularity are as follows

$$\text{ES:}\quad \left.\frac{\partial^2 w}{\partial \tilde{r}^2}\right|_{r^*} < 0 \quad\Leftrightarrow\quad f''(r^*) < \frac{2}{r^{*2}(r^* + f(r^*) - 1)} - \frac{8}{r^{*2}(r^* + f(r^*) - 1)^3}, \tag{A.18}$$

$$\text{CS:}\quad \left.\frac{\partial^2 w}{\partial \tilde{r}^2} + \frac{\partial^2 w}{\partial r\,\partial \tilde{r}}\right|_{r^*} < 0 \quad\Leftrightarrow\quad f''(r^*) < \frac{2}{r^{*2}(r^* + f(r^*) - 1)} - \frac{8}{r^{*2}(r^* + f(r^*) - 1)^3} + \frac{2(r^* + f(r^*) + 1)}{r^{*2}(r^* + f(r^*) - 1)^3}. \tag{A.19}$$

Appendix B

The ES and CS boundary can be computed analytically in the region of 2-cycles and 4-cycles (see main text) but not for periodic regions beyond 4-cycles. To determine the boundaries in other periodic regions we use the method of trade-off invasion plots (TIPs, Bowers et al. 2005) and a numerical scheme to determine the invasion boundaries on the TIP. The method of TIPs allows the values of the singular point to be specified and then determines the invasion boundaries relative to the singular point. For Fig. 2, we choose $s = 0.6$ and vary r and solve for the invasion boundaries at each value of r. A numerical procedure is used to determine the values of $\tilde{r}$ for which

the fitness function $w(\tilde{r}, r) = 0$ (see (10)) for two values of $\tilde{s}$ close to the singular point. We then fit a quadratic curve, $\tilde{s} = A_1\tilde{r}^2 + B_1\tilde{r} + C_1$ to pass through the singular point (r^*, s^*) and the two nearby points where the fitness function is zero. This approximates the $w(\tilde{r}, r) = 0$ invasion curve close to the singular point. In a similar manner we can find points close to the singular point where $w(\tilde{r}, r) = 0$ and approximate this invasion curve as $\tilde{s} = A_2\tilde{r}^2 + B_2\tilde{r} + C_2$ in the neighbourhood of the singular point. The method of TIPS shows that the ES boundary is equivalent to the $w(\tilde{r}, r) = 0$ curve and hence $f''(r) = 2A_1$ defines the corresponding boundary in Fig. 2(b); similarly the CS boundary is equivalent to the vertical average of the two invasion curves and hence $f''(r) = A_1 + A_2$ defines the appropriate boundary here in Fig. 2(b). A comparison of this numerical method and the analytical method in the 2-cycle and 4-cycle region gives an excellent fit and the numerical method is used to determine the ES and CS boundaries for periodic regions beyond 4-cycles. This method could be used in other models where analytical results cannot be determined for non-equilibrium dynamics. A cautionary note is that the points close to the singular point must be chosen carefully such that all points lie on the 'same' attractor (an attractor with the same period) as, if the points lie on different attractors, this method fails. The method cannot be used in the chaotic parameter region as it is not possible to select a consistent attractor near to the singular point.

Appendix C

Simulation analysis is used to verify the theoretical results about the position and nature of the singular point. In the simulations, the population dynamics were numerically solved for a fixed time (t_a) according to (1) initially with a monomorphic population. Mutant strains, those we defined by trait values $\tilde{r}$ (and $\tilde{s} = f(\tilde{r})$), were generated by small deviations around the current trait r (and $s = f(r)$) (the choice of current strain from which to mutate depends on its relative density) and introduced at low density. The population dynamics were then solved for a further time t_a with strains whose population density fell below a (low) threshold considered extinct and removed before considering new mutations and repeating the procedure. In this way, the parameter r (and therefore s via the trade-off) could evolve. One difference between the theory and simulations is that the simulations are not mutation-limited (i.e. new mutants could evolve before previous mutants had reached equilibrium or gone extinct). Although this could be overcome by increasing t_a, this set-up has been shown to correctly approximate the evolutionary behaviour predicted by adaptive dynamics in studies where the dynamical attractor is an equilibrium point (see, for example, White and Bowers 2005; White et al. 2006).

References

Boldin, B., Geritz, S. A. H., & Kisdi, É. (2009). Superinfections and adaptive dynamics of pathogen virulence revisited: a critical function analysis. *Evol. Ecol. Res.*, *11*, 153–175.

Boots, M., & Haraguchi, Y. (1999). The evolution of costly resistance in host-parasite systems. *Am. Nat.*, *153*, 359–370.

Bowers, R. G., White, A., Boots, M., Geritz, S. A. H., & Kisdi, E. (2003). Evolutionary branching/speciation: contrasting results from systems with explicit or emergent carrying capacities. *Evol. Ecol. Res.*, *5*, 883–891.

Bowers, R. G., Hoyle, A., White, A., & Boots, M. (2005). The geometric theory of adaptive evolution: trade-off and invasion plots. *J. Theor. Biol.*, *233*, 363–377.

Cushing, J. M., Costantino, R. F., Dennis, B., Desharnais, R. A., & Henson, S. M. (2003). *Chaos in ecology [electronic resource]: experimental nonlinear dynamics*. Amsterdam: Academic Press.

De Mazancourt, C., & Dieckmann, U. (2004). Trade-off geometries and frequency-dependent selection. *Am. Nat.*, *164*, 765–778.

Doebeli, M., & Koella, J. C. (1995). Evolution of simple population-dynamics. *Proc. R. Soc. Lond. Ser. B, Biol. Sci.*, *260*, 119–125.

Ebenman, B., Johansson, A., Jonsson, T., & Wennergren, U. (1996). Evolution of stable population dynamics through natural selection. *Proc. R. Soc. Lond., Ser. B, Biol. Sci.*, *263*, 1145–1151.

Eckmann, J. P., & Ruelle, D. (1985). Ergodic-theory of chaos and strange attractors. *Rev. Mod. Phys.*, *57*, 617–656.

Ferriere, R., & Gatto, M. (1993). Chaotic population-dynamics can result from natural-selection. *Proc. R. Soc. Lond., Ser. B, Biol. Sci.*, *251*, 33–38.

Gatto, M. (1993). The evolutionary optimality of oscillatory and chaotic dynamics in simple population-models. *Theor. Popul. Biol.*, *43*, 310–336.

Geritz, S. A. H., Kisdi, E., Meszena, G., & Metz, J. A. J. (1998). Evolutionarily singular strategies and the adaptive growth and branching of the evolutionary tree. *Evol. Ecol.*, *12*, 35–57.

Geritz, S. A. H., Kisdi, E., & Yan, P. (2007). Evolutionary branching and long-term coexistence of cycling predators: critical function analysis. *Theor. Popul. Biol.*, *71*, 424–435.

Greenman, J. V., Benton, T. G., Boots, M., & White, A. R. (2005). The evolution of oscillatory behavior in age-structured species. *Am. Nat.*, *166*, 68–78.

Gurney, W. S. C., & Nisbet, R. M. (1998). *Ecological dynamics*. New York: Oxford University Press.

Katok, A., & Hasselblatt, B. (1995). *Introduction to the modern theory of dynamical systems*. Cambridge: Cambridge University Press.

Kisdi, E. (2001). Long-term adaptive diversity in Levene-type models. *Evol. Ecol. Res.*, *3*, 721–727.

Levins, R. (1962). Theory of fitness in a heterogeneous environment 1. Fitness set and adaptive function. *Am. Nat.*, *96*, 361.

May, R. M. (1975). Deterministic models with chaotic dynamics. *Nature*, *256*, 165–166.

Metz, J. A. J., Nisbet, R. M., & Geritz, S. A. H. (1992). How should we define fitness for general ecological scenarios. *Trends Ecol. Evol.*, *7*, 198–202.

Metz, J. A. J., Geritz, S. A. H., Meszena, G., Jacobs, F. J. A., & Van Heerwaarden, J. S. (1996). Adaptive dynamics: a geometric study of the consequences of nearly faithful reproduction. In: S.J.M. Van Strien & S.M. Verduyn Lunel (Eds.), *Stochastic and spatial structures of dynamical systems* (pp. 183–231). Amsterdam: North-Holland.

Mueller, L. D., Joshi, A., & Borash, D. J. (2000). Does population stability evolve? *Ecology*, *81*, 1273–1285.

Prasad, N. G., & Joshi, A. (2003). What have two decades of laboratory life-history evolution studies on Drosophila melanogaster taught us? *J. Genet.*, *82*, 45–76.

Roff, D. A. (2002). *Life history evolution*. Sunderland: Sinauer Associates.

Rueffler, C., Van Dooren, T. J. M., & Metz, J. A. J. (2004). Adaptive walks on changing landscapes: Levins' approach extended. *Theor. Popul. Biol.*, *65*, 165–178.

Schaffer, W. M. (1974). Selection for optimal life histories—effects of age structure. *Ecology*, *55*, 291–303.

Stearns, S. C. (1992). *The evolution of life histories*. Oxford: Oxford University Press.

Svennungsen, T. O. & Kisdi, É. (2009). Evolutionary branching of virulence in a single infection model. *J. Theor. Biol.*, *257*, 408–418.

White, A., & Bowers, R. G. (2005). Adaptive dynamics of Lotka-Volterra systems with trade-offs: the role of interspecific parameter dependence in branching. *Math. Biosci.*, *193*, 101–117.

White, A., Greenman, J. V., Benton, T. G., & Boots, M. (2006). Evolutionary behaviour in ecological systems with trade-offs and non-equilibrium population dynamics. *Evol. Ecol. Res.*, *8*, 387–398.